



HAL
open science

Fault diagnosis for fuel cell systems: A data-driven approach using high-precise voltage sensors

Zhongliang Li, Rachid Outbib, Stefan Giurgea, Daniel Hissel, Alain Giraud,
Pascal Couderc

► **To cite this version:**

Zhongliang Li, Rachid Outbib, Stefan Giurgea, Daniel Hissel, Alain Giraud, et al.. Fault diagnosis for fuel cell systems: A data-driven approach using high-precise voltage sensors. *Renewable Energy*, 2018, 135, pp.1435-1444. 10.1016/j.renene.2018.09.077 . hal-02004101

HAL Id: hal-02004101

<https://amu.hal.science/hal-02004101>

Submitted on 12 Feb 2020

HAL is a multi-disciplinary open access archive for the deposit and dissemination of scientific research documents, whether they are published or not. The documents may come from teaching and research institutions in France or abroad, or from public or private research centers.

L'archive ouverte pluridisciplinaire **HAL**, est destinée au dépôt et à la diffusion de documents scientifiques de niveau recherche, publiés ou non, émanant des établissements d'enseignement et de recherche français ou étrangers, des laboratoires publics ou privés.



Distributed under a Creative Commons Attribution - NonCommercial - NoDerivatives 4.0
International License

Fault diagnosis for fuel cell systems: A data-driven approach using high-precise voltage sensors

Zhongliang Li^{a,b,c,*}, Rachid Outbib^a, Stefan Giurgea^{b,c}, Daniel Hissel^{b,c},
Alain Giraud^d, Pascal Couderc^e

^a*Aix Marseille Univ, Universit de Toulon, CNRS, LIS, Marseille, France*

^b*FCLAB (Fuel Cell Lab) Research Federation, FR CNRS 3539, rue Thierry Mieg, 90010 Belfort Cedex, France*

^c*FEMTO-ST (UMR CNRS 6174), ENERGY Department, UFC/UTBM/ENSMM, France*

^d*CEA/LIST, 91191 Gif-sur-Yvette Cedex, France*

^e*3D PLUS, 78532 BUC, France*

Abstract

Reliability and durability are two key hurdles that prevent the widespread use of fuel cell technology. Fault diagnosis, especially online fault diagnosis, has been considered as one of the crucial techniques to break through these two bottlenecks. Although a large number of works dedicated fuel cell diagnosis have been published, the criteria of diagnosis, especially online diagnosis have not yet been clarified. In this study, we firstly propose the criteria used for evaluating a diagnosis strategy. Based on that, we experimentally demonstrate an online fault diagnosis strategy designed for Proton Exchange Membrane Fuel Cell (PEMFC) systems. The diagnosis approach is designed based on advanced feature extraction and pattern classification techniques,

*Corresponding author. Tel.: +33 (0)4 91 05 60 32, Fax: +33 (0)4 91 05 60 33. E-mail address: zhongliang.li@lisis.org (Z. LI), rachid.outbib@lisis.org (R. OUTBIB), stefan.giurgea@utbm.fr (S. GIURGEA), daniel.hissel@univ-fcomte.fr (D. HISSEL), alain.giraud@cea.fr (A. GIRAUD), pcouderc@3d-plus.com (P. COUDERC)

and realized by processing individual fuel cell voltage signals. We also develop a highly integrated electronic chip with multiplexing and high-speed computing capabilities to fulfill the precise measurement of multi-channel signals. Furthermore, we accomplish the diagnosis algorithm in real-time. The excellent performance in both diagnosis accuracy and speediness over multiple fuel cell systems is verified. The proposed strategy is promising to be utilized in various fuel cell systems and promote the commercialization of fuel cell technology.

Keywords: PEMFC system, Fault diagnosis, Application specific integrates circuit, Data-driven, Classification, Online implementation

1. Introduction

Fuel cell technology, because of its potential for effectively alleviating environmental and resource issues, has been attracting considerable increasing attention. Among the various fuel cells, proton exchange membrane fuel cell (PEMFC), thanks to its high power density and efficiency, low operating temperature, and quick response to load, is the most promising one to be widely applied in both stationary and automotive cases. However, reliability and durability are currently two main barriers which prevent the process for its wide applications [1, 2]. Among the solutions, fault diagnosis, more particularly online diagnosis, dedicated to detecting, isolating, and analyzing different faults, has proved to be beneficial for keeping fuel cell systems operating safely, reducing downtime and mitigating performance degradation [3, 4, 5].

The operation of a PEMFC system involves multiple auxiliary subsystems

15 other than fuel cell stack, and requires multi-field knowledge, for example
16 complex electrochemistry, thermodynamics, and fluid mechanics. To accu-
17 rately detect and identify the faults occurring in the system is not a trivial
18 task. During the last decade, considerable attention has been focused on the
19 topics related to fault diagnosis for PEMFC systems.

20 Among the most substantial approaches, model based fault diagnosis ap-
21 proaches have been proposed. A review of model based methods is available
22 in [6]. Most of these approaches are based on some general input-output
23 or state space models, which are usually developed from the physical and
24 mathematical knowledge of the process [7]. In [8], the authors developed
25 an electrical equivalent circuit which can be seen as an analytical model of
26 the concerned PEMFC system. The component parameters are identified
27 and the variation of the specific electrical component values can be seen as
28 the indicator of the corresponding faults. In [9], a linear parameter vary-
29 ing (LPV) model is built for a commercial PEMFC system. An observer
30 is proposed based on the proposed LPV model. Then, the residuals can
31 be computed by comparing the process outputs and the outputs estimated
32 from the observer. The similar methods are also used in [10, 11]. Besides
33 designing a specific observer, the parity relation is also used for residual
34 generation procedure in a more straightforward way [12]. To carry out the
35 above mentioned three kinds of analytical model based approaches, an accu-
36 rate process model of PEMFC systems is necessary. However, modeling the
37 PEMFC systems is a rather difficult task. Especially, the identification of
38 fuel cell inner parameters concerning the operation, the geometries as well
39 as the materials is difficult [13]. Even the parameters are identified, some of

40 them are time-varying because of the ageing degradation. In addition, the
41 existing models are usually not able to fulfill sufficient accuracy, generaliza-
42 tion and real-time implementability, which makes model based approaches
43 insufficiently suitable for wide practical applications [14].

44 Another branch named data-driven diagnosis has been gaining increasing
45 attention. The data-driven methods are those make use of the information
46 from the historical data other than an analytical model. A review of data-
47 driven methods is available in [4]. In [15], [16], and [17], fuzzy inference and
48 neural networks are used to build “black-box” models whose parameters are
49 obtained by fitting the experimental data obtained in fault free state. With
50 these “black-box” models, the diagnosis can be realized by evaluating the
51 difference between the real system outputs and the model outputs. In [18], a
52 multivariate analysis technique, named principal component analysis (PCA),
53 is used for diagnosis by analyzing the variables measured by multiple sensors
54 installed in a PEMFC system. In [19], the fuzzy clustering method is used to
55 process the signals acquired from a commercial PEMFC system in order to
56 achieve fault diagnosis. In [20] and [21], Bayesian networks classification is
57 used for the PEMFC diagnosis. In [22], [23], and [24], the signal processing
58 methods, fast fourier transform, wavelet transformation, multifractal formal-
59 ism, are respectively used to extract the features which are sensitive to faults
60 from the fuel cell stack voltage signals. Although some interesting prelimi-
61 nary results have been proposed in the frame of data-driven diagnosis, the
62 online validation of those approaches in different real PEMFC systems has
63 not yet been announced.

64 Actually, some criteria have to be satisfied to realize online diagnosis for

65 PEMFC systems serving in real conditions. First, the sensors for measuring
66 the variables serving as the inputs of the fault diagnosis approach should be
67 minimized and arranged in limited space. The intrusive and/or costly sensors
68 or instruments should be avoided whenever possible. Second, the diagnosis
69 accuracy should be maintained at a high level with respect to different faults
70 and different PEMFC systems. Third, the online diagnosis approach needs
71 to be computationally efficient since it is usually implemented in some “on-
72 board” embedded system with limited computational power available [25, 26].
73 Fourth, because of ageing effects, fuel cells’ behaviors are time-variant. The
74 diagnosis approach should be capable of being adapted online. In addition,
75 the serial-connected single fuel cells which compose a fuel cell stack are usu-
76 ally considered to be identical in the existing approaches. Nevertheless, the
77 inhomogeneity among cells should be more emphasized when we talk about
78 “faults”. This is because usually a proportion of fuel cells fall into faulty
79 state first when a fault occurs [27, 28].

80 In this article, we propose and experimentally demonstrate an online fault
81 diagnosis strategy for PEMFC systems. To achieve the diagnosis goal, we de-
82 signed an reduced volume application specific integrates circuit (ASIC) which
83 integrate multichannel voltage sensors of giant magneto resistance (GMR)
84 type, and a field programmable gate array (FPGA) based computing unit
85 [29, 30]. The individual fuel cell voltages can be precisely measured and
86 treated as the input variables of the diagnosis approach. The discriminant
87 features are extracted using fisher discriminative analysis (FDA) from the
88 vectors composed by cell voltages and classified the features using support
89 vector machine (SVM) into different classes that represent different states of

90 health. Besides the requirements for a basic diagnosis approach, the novel
91 fault detection and online adaptation functions are also developed and added
92 to the proposed approach. They are realized through using specifically de-
93 signed diagnosis rules and an incremental learning method. We verified the
94 efficiency of our strategy via the experiments on several stacks and multiple
95 faulty types. To our knowledge, this work is the first to provide a high-
96 performance online diagnosis strategy implemented in an ASIC for PEMFC
97 systems.

98 The rest of the paper is organized as follows: the development process of
99 the proposed diagnosis strategy is given in Section 2. Section 3 and Section 4
100 present respectively the diagnosis approach and the ASIC designed to realize
101 diagnosis function. Experimental platform and database preparation are
102 described in Section 5. Diagnosis results are summarized and analyzed in
103 Section 6. We finally conclude the work in Section 7.

104 **2. Diagnosis strategy development process**

105 The proposed data-driven diagnosis strategy consists of offline and online
106 stages (see Fig. 1(a)). The feature extraction (FDA) and the classification
107 models (SVM) are trained and tested offline. The objective of the test stage
108 is to optimize the parameters used for SVM. The trained models are imple-
109 mented online to achieve the diagnosis goal. Moreover, based on the data
110 sampled online, the SVM model can be adapted online.

111 The realization process is shown in Fig. 1(b). In the offline stage, the
112 historical data (individual cell voltages) are measured using the GMR sensors
113 integrated in the ASIC and saved as the training and test database into a

114 PC. Then the diagnosis model is trained using the PC and programmed into
115 the memory of the ASIC. In the online stage, the variables (individual cell
116 voltages) are measured and processed using the ASIC with the model trained
117 offline.

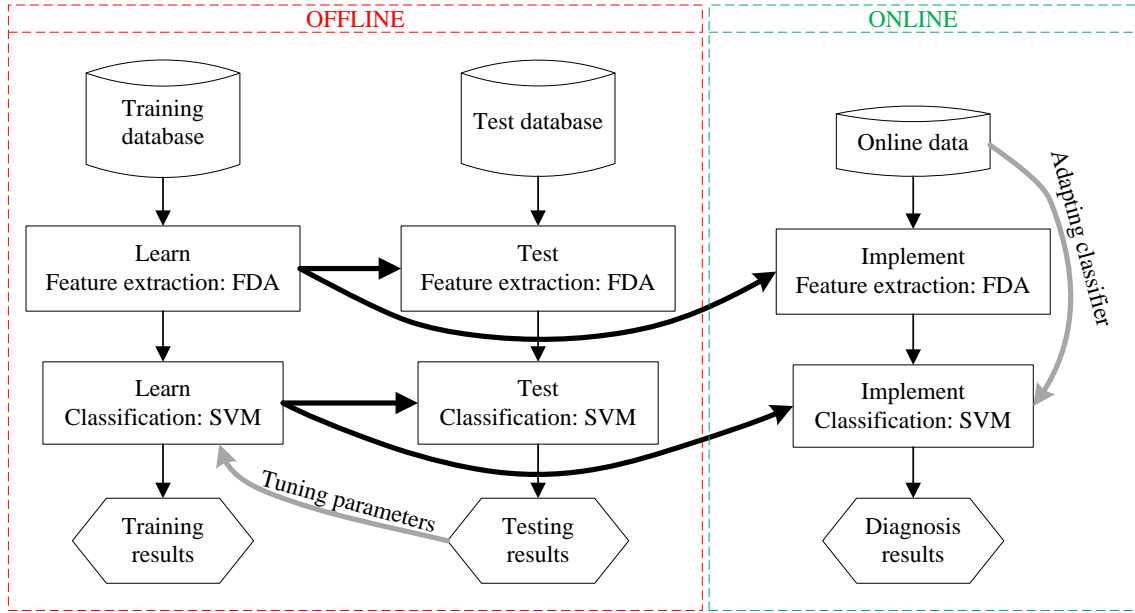
118 **3. Diagnosis approach**

119 In this section, the diagnosis problem and the involved methodologies are
120 presented mathematically in a general manner. Actually, the main focus of
121 this paper is to provide the completed implementation process of the pro-
122 posed diagnosis strategy, which includes both software and hardware devel-
123 opments. The mathematical details of the involved algorithms are provided
124 by citing several published works.

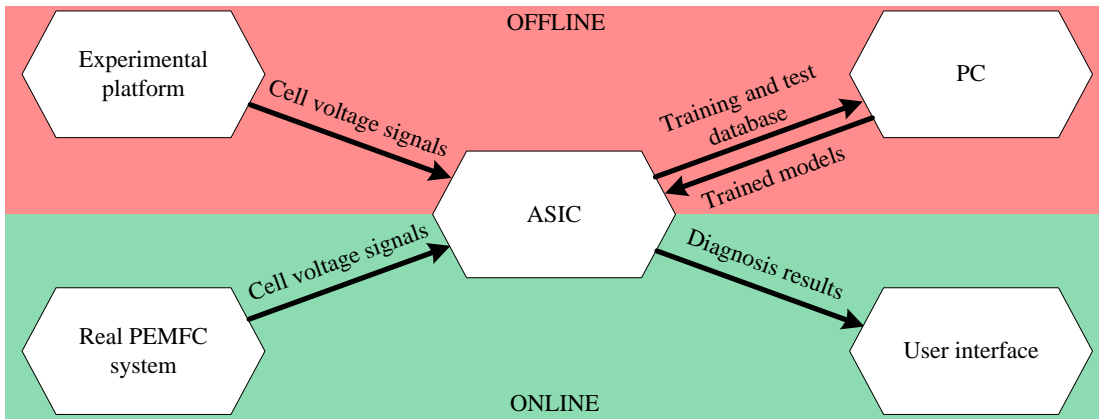
125 *3.1. Problem formulation*

126 The diagnosis approach proposed in this study belongs to the category of
127 supervised methods. The basic tasks of fault diagnosis, i.e. fault detection
128 and isolation, can be abstracted as a typical pattern classification problem
129 (see Fig. 2).

130 Suppose that the fuel cell stack in a concerned system is composed of M
131 single fuel cells. At a certain time, the individual cell voltages are measured
132 and denoted as a vector $\mathbf{v} = [v_1, v_2, \dots, v_M]^T$. Suppose that we have a training
133 dataset \mathbf{V} which consists of N such vectors, i.e. $\mathbf{V} = \{\mathbf{v}_1, \mathbf{v}_2, \dots, \mathbf{v}_N\}$. These
134 vectors are known to be distributed in the classes denoted as $\Omega_0, \Omega_1, \Omega_2, \dots,$
135 Ω_C , in which the class label 0 corresponds to the fault free state, while 1, 2,
136 \dots, C correspond to the faults of various types. The class label g_i of vector
137 \mathbf{v}_i is known in prior. Based on the dataset \mathbf{V} , a function denoted as $F(\cdot)$



(a)



(b)

Figure 1. Diagram of the proposed diagnosis approach and of the realization process. (a) Workflow of the proposed diagnosis approach. (b) Realization process of the diagnosis strategy.

138 can be trained offline. Through the function, the class label of a given vector
 139 formed by the cell voltages can be determined as

$$g_n = F(\mathbf{v}_n) \quad (1)$$

140 The diagnosis procedure is the process of implementing this function online.

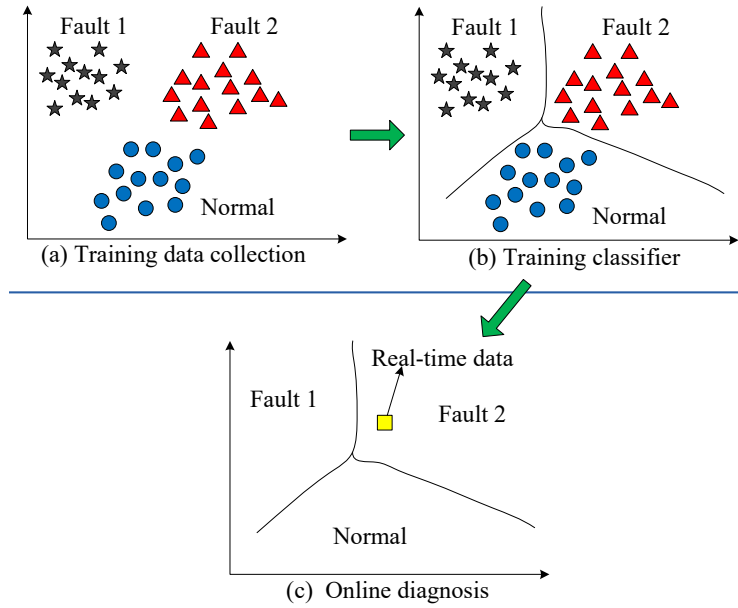


Figure 2. Principle of classification based fault diagnosis. The implementation of the approach can be divided into three steps. (a) The historical data in both health state and concerned faulty states are collected as the training data base. In this case, the data are distributed in three classes: normal, fault 1 and fault 2. (b) A classifier is trained based on the training data base. The trained classifier is described as the boundaries among the classes. (c) The trained classifier is performed online. According to the classifier or the boundaries here, an arbitrary online sample is classified into one of the concerned classes. Fault detection and isolation is thus realized. In this case, the online sample is classified into fault 2 class.

141 A large dimensional number M , i.e. the single fuel cell number, may

142 cause a heavy burden of online computation and a reduced diagnosis power.
 143 We therefore propose a two-step diagnosis procedure to solve the problem as
 144 follows: a feature extraction stage to reduce the original data dimensional
 145 number is carried out first, as

$$\mathbf{z}_n = f_1(\mathbf{v}_n) \quad (2)$$

146 where \mathbf{z}_n is a L -dimensional vector composed of features ($L < M$). Then,
 147 the classification is implemented in the feature space as

$$g_n = f_2(\mathbf{z}_n) \quad (3)$$

148 Such that the diagnosis procedure is transformed into a two-step proce-
 149 dure. By comparing several representative feature extraction and classifica-
 150 tion methods from the point of view of diagnosis precision and computational
 151 complexity, FDA and SVM methods were selected as the feature extraction
 152 and classification tools, respectively [31].

153 3.2. Principle of FDA

154 FDA is a supervised technique developed to extract the features from the
 155 data in the hope of obtaining a more manageable classification problem [32].
 156 The objective of FDA is to project the data into a lower dimensional space
 157 in which the variance between classes is maximized while the variance within
 158 an identical class is minimized. Through the training process, C projecting
 159 vectors (C fault types in the training dataset), denoted as $\mathbf{w}_1, \mathbf{w}_2, \dots, \mathbf{w}_C$,
 160 can be determined in the offline training phase. The features of the vector
 161 \mathbf{v}_n can be computed as $\mathbf{z}_n = [\mathbf{w}_1^T \mathbf{v}_n, \mathbf{w}_2^T \mathbf{v}_n, \dots, \mathbf{w}_C^T \mathbf{v}_n]^T$. The details on FDA
 162 implementation can be found in [31].

163 *3.3. Principle of SVM*

164 SVM is a classification method developed originally by V. Vapnik in 1998
165 and has been considered as the present state of art classifier [33]. SVM func-
166 tions by projecting the data into a high-dimensional space and constructing
167 a hyperplane which separates the cases of different classes in this space.
168 Different from the basic SVM, spherical shaped multi-class support vector
169 machine (SSM-SVM), considered as a modified version, was employed in our
170 approach [34]. The principle of SSM-SVM is to project the original data
171 into a high-dimensional space and seek multiple class-specific spheres which
172 enclose the samples from an identical class while excluding those from the
173 other classes in this space (see Fig. 3). The projection from original space to
174 high-dimensional space and some data processing are realized by introducing
175 a kernel function and playing “kernel trick”. Training a SVM classifier can be
176 finally abstracted as a quadric problem, while implementing a SVM classifier
177 involves a small proportion of the training data which are named “support
178 vectors”.

179 To determine the class label of a sample \mathbf{z}_n , the following criterion is used

$$g_n = \arg \max_i G_i(d_i(\mathbf{z}_n)) \quad i = 0, 1, 2, \dots, C \quad (4)$$

180 where G_i is a smooth monotonous decreasing function, $d_i(\mathbf{z}_n)$ is the distance
181 from \mathbf{z}_n to the i th sphere center and it can be calculated based on training
182 result. See [14] for more details of SSM-SVM classification.

183 *3.4. Diagnosis rules*

184 A conventional classification method can only classify a sample into a
185 known class. It will lose its efficiency as a sample comes from a novel class,

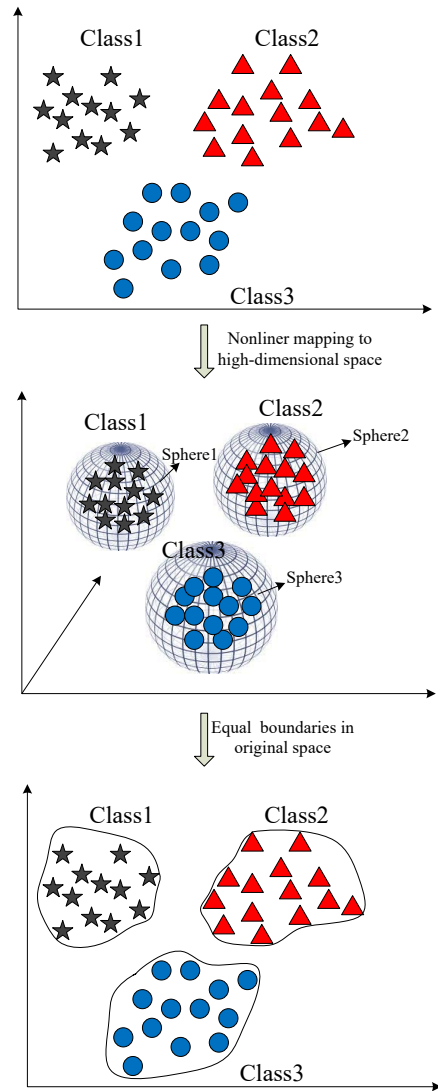


Figure 3. Principle of SSM-SVM classification. The training data are distributed in three classes labeled by class 1, class 2 and class 3. Through nonlinear mapping, the original data are projected into high-dimensional space (3-dimension in this case). In the high-dimensional space, the class-specific spheres can be found through training. The class-specific spheres enclose the samples from a specific class, while excluding those from the other classes. These spheres can be seen as the class-specific boundaries in the original space.

186 i.e. a novel faulty mode in our case. In order to recognize the novel faulty
 187 mode, we propose to set boundaries for the spheres in high-dimension space.
 188 The samples from a novel cluster can thus be detected if they are outside all
 189 the closed boundaries. To realize this, the function G_i in terms of $d_i(\mathbf{z})$ is
 190 defined as

$$G_i(d_i(\mathbf{z})) = \begin{cases} 0.5 \left(\frac{1 - d_i(\mathbf{z})/R_i}{1 + \zeta_1 d_i(\mathbf{z})/R_i} \right) + 0.5 & \text{if } d_i(\mathbf{z}) \leq R_i \\ 0.5 \left(\frac{1}{1 + \zeta_2(d_i(\mathbf{z}) - R_i)} \right) & \text{otherwise} \end{cases} \quad (5)$$

191 where R_i is the radius of i th sphere, ζ_1 and ζ_2 are constants that satisfy
 192 $R_i \zeta_2(1 + \zeta_1) = 1$. It could be proved that $G_i : \mathbb{R}_+ \rightarrow \mathbb{R}_+$ is a smooth
 193 decreasing function with $\lim_{\tau \rightarrow \infty} G_i(\tau) = 0$.

194 It is considered that a sample \mathbf{z} belongs more probably to the class with
 195 the shortest distance from the sphere center to the sample. However, if this
 196 distance is still larger than a threshold, we will consider the sample is from
 197 a novel class (novel fault mode). Mathematically, the diagnosis rule is

$$g_n = \begin{cases} \arg \max_i G_i(d_i(\mathbf{z})) & \text{if } \max_i G_i(d_i(\mathbf{z})) \geq \delta_i \\ \text{new} & \text{if } \max_i G_i(d_i(\mathbf{z})) < \delta_i \end{cases} \quad (6)$$

198 where the threshold δ_i is determined based on a calibration dataset with N_i
 199 elements, and a way to fix its value is to use the *3-sigma law*:

$$\delta_i = M_i - 3 \sqrt{\frac{1}{N_i} \sum_{g_n=i} (G_i(d_i(\mathbf{z})) - M_i)^2} \quad (7)$$

200 with $M_i = \frac{1}{N_i} \sum_{g_n=i} G_i(d_i(\mathbf{z}_n))$.

201 3.5. Online adaptation method

202 Traditional SVM training is performed in one data batch and it must
 203 be redone from scratch if the training dataset varies. The computational

204 cost for the training procedure is usually heavy and realized offline. To
205 realize online updating of the classifier as time goes on, we propose here an
206 incremental learning method for training the proposed SSM-SVM [14]. In
207 this method, the solution for $N+1$ training data could be formulated in terms
208 of the solution for N data and one new data point. The light computational
209 complexity makes the incremental learning procedure suitable for online use.
210 The theoretical deduction of incremental learning can be found in [14].

211 **4. ASIC developed for implementing the diagnosis approach**

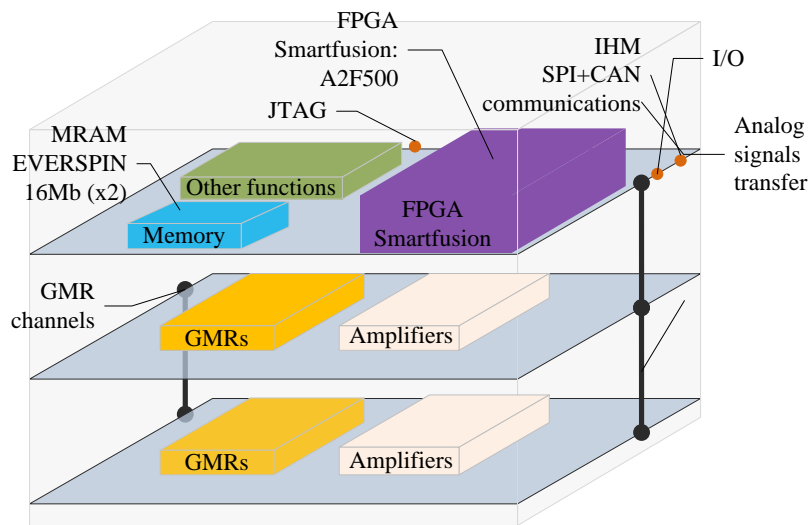
212 Since the input variables for the diagnosis approach we propose are in-
213 dividual cell voltages, a sensor capable of precisely measuring the voltage
214 signals of low amplitude and multiplexing is required. We propose here an
215 integrated voltage sensor which is based on GMR technology [29]. Compared
216 with the traditional Hall effect sensors which are commonly used for voltage
217 or current measurement, the GMR sensors exhibit a much higher sensitivity
218 especially in low current (voltage), high precision applications [35]. Knowing
219 that a single cell voltage is usually less than 1 V, GMR sensors are well suited
220 in our case. Moreover, the sensor developed here also improves the present
221 state of the art in the aspects of increasing insulation capability ($> 2000kV$)
222 [36].

223 To implement the proposed diagnosis approach, multiple GMR voltage
224 sensors are packaged with a commercial system on chip (SoC) FPGA device
225 which functions as the computation and communication unit. As shown in
226 Fig. 4(a), these components are designed in the form of a 3D integration cir-
227 cuit. The upper layer taking charge of computation and communication can

228 be seen as the “main board”. In this layer, the Smartfusion on-chip system
229 developed by Microsemi is integrated. The device integrates an FPGA fab-
230 ric, an ARM Cortex-M3 Processor, and programmable analog circuitry. The
231 ARM Cortex-M3 processor is an 100 MHz, 32-bit CPU. The programmable
232 analog circuitry can function as the D/A and A/D conversion blocks. This
233 integrated device is equipped with up to 512 KB flash and 64 KB of SRAM.
234 Besides, another two 16 M memory chips is added to the system. With the
235 abundant connecting ports, different kinds of communications can be realized
236 with other devices. The other two layers, which are equipped with GMR sen-
237 sors, are adapted for measuring multi-channel voltage signals precisely. The
238 appearance of the 3D ASIC and the test board are shown respectively in Fig.
239 4(b) and Fig. 4(c).

240 5. Database preparation

241 In order to generate the database for training and testing the diagnosis
242 model as well as validating the performance of online implementation, we
243 carried out a series of experiments including the ones under normal operating
244 condition and faulty conditions. The faults created deliberately cover the
245 abnormal operations in different components of a PEMFC system, such as
246 the water management subsystem, the temperature management subsystem,
247 the electric circuit, the air and hydrogen circuits. The faults studied are
248 usually considered as “reversible” or “recoverable”, which means they can be
249 corrected through appropriate operations and do not cause the permanent
250 defects in the systems. Actually, accurate diagnosis of this kind of faults can
251 usually avoid the occurrence of those so-called permanent faults. During the



(a)



(b)



(c)

Figure 4. ASIC designed for monitoring individual fuel cell voltages and implementing the diagnosis approach. (a) The architecture of the ASIC, which was specially designed for the PEMFC system diagnosis. (b) The appearance of the designed ASIC. The ASIC is with compact package dimensions of $27 \times 27 \times 12 \text{ mm}^3$. (c) The ASIC is installed into a printed circuit board (PCB) which is equipped with the connectors, test points and LED lights.

252 experiments the data were captured using the designed ASIC and saved into
253 the disk of a PC.

254 *5.1. PEMFC platform*

255 A 1 kW and a 10 kW experimental platform, which had been developed
256 in-lab, were employed to fulfill the experimental requirements (see Fig. 5).
257 In the hydrogen and air circuits, the temperatures, pressures, flow rates, and
258 relative humidifies can be regulated in a wide range. A thermal-regulated
259 water circuit ensures the flexible control of the stack temperature. The load
260 current profile can be defined or simulated with the help of a DC electronic
261 load. A terminal is installed into the stack to facilitate the connection to the
262 ASIC and to monitor the cell voltages.

263 The platform enables us to emulate different faults artificially, and thus
264 generate the database for both offline training and online validation. In or-
265 der to verify the generalization performance of the proposed approach, three
266 stacks from different industrial suppliers and with different cell numbers,
267 power levels, mechanical designs were explored respectively on the two plat-
268 forms (Fig. 6).

269 *5.2. Concerned faults*

270 Thanks to the home-made platforms in which a number of operating
271 parameters can be set flexibly, we experimentally simulated a variety of faults
272 that can potentially occur in different components of a PEMFC system.
273 In order to cover the possible fault types, 7 fault types involving different
274 subsystems or components were explored in this study. These faults and
275 corresponding operations are summarized in Table 3. In addition to the

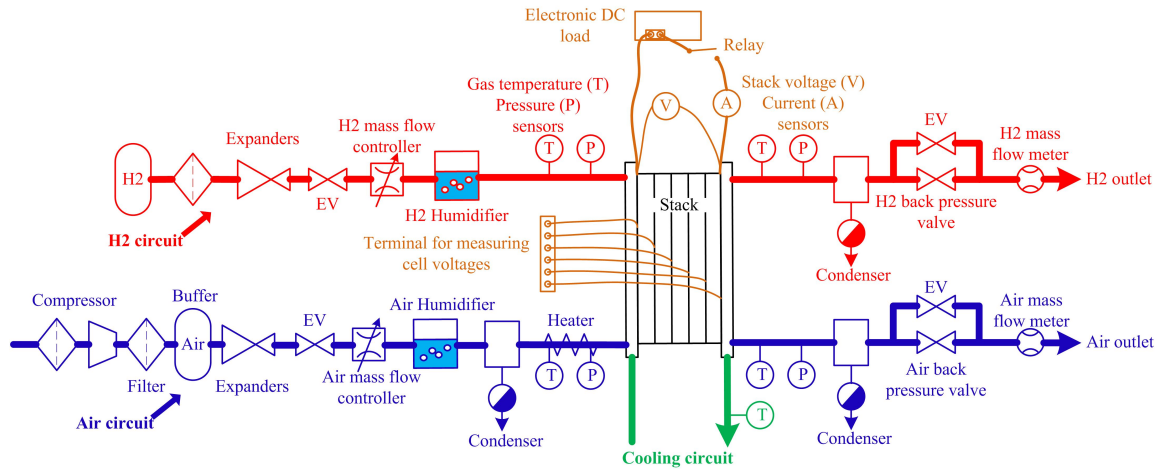


Figure 5. Schematic of the platforms used for generating the training and test database and for online validation.

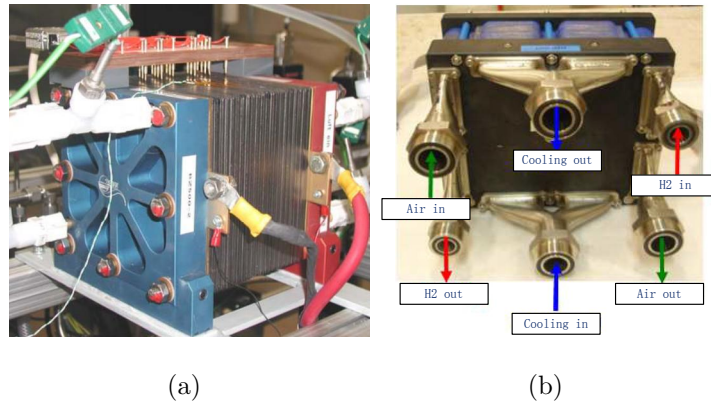


Figure 6. (a) 20-cell stack installed in the platform. (b) Appearance of the 8-cell stack and 40-cell stack.

Table 1. Technical parameters of the 20-cell stack

Parameter	Value
Active area	100 cm ²
Flow field structure	serpentine
Electrode surface area	100 cm ²
Nominal output power	500 W
Operating temperature region	20-65 °C
Maximum operating pressures	1.5 bar
Anode stoichiometry	2
Cathode stoichiometry	4

276 individual cell voltages, a detailed measurements of temperatures, current,
 277 pressures and gas flow rates have been achieved thanks to the well-equipped
 278 platforms. In this study, the importance is put on the combination of ASIC
 279 and data-driven diagnosis approach and their implementation for various fuel
 280 cell stacks. The detailed waveforms and analysis of the acquired data during
 281 each fault experiment have been summarized in the previous articles [37] [28]
 282 [38].

283 6. Results

284 We carried out a number of experiments in both normal operating and
 285 faulty cases to collect the data for training and testing the proposed diagnosis
 286 model. Then, the trained diagnosis model was programmed into the memory
 287 of the ASIC and implemented online.

Table 2. Technical parameters of the 8-cell stack and 40-cell stack

Parameter	Value
Active area	200 cm ²
Stoichiometry H_2	1.5
Stoichiometry <i>Air</i>	2
Pressure at H_2 inlet	150 kPa
Pressure at <i>Air</i> inlet	150 kPa
Pressure differential between anode and cathode	30 kPa
Temperature (exit of cooling circuit)	80 °C
Anode relative humidity	50%
Cathode relative humidity	50%
Current	110 A
Voltage per cell	0.7 V
Electrical power of 8-cell stack	616 W
Electrical power of 40-cell stack	3080 W

Table 3. Experiments on various health states carried out on different PEMFC stacks

Stack	Health state description	Location	Operation	Notation
20-cell stack	Normal operating	Whole system	Nominal operation	<i>Normal</i>
	Flooding	Water management subsystem	Increase air relative humidity	F_1
	Membrane drying	Water management subsystem	Deactivate air humidifier	F_2
8-cell stack	Normal operating	Whole system	Nominal operation	<i>Normal</i>
	High current pulse	Electric circuit	Short circuit	F_3
	High temperature	Temperature subsystem	Stop cooling water	F_4
	High air stoichiometry	Air supply subsystem	Increase air stoichiometry to 2.0 normal value	F_5
	Low air stoichiometry	Air supply subsystem	Decrease air stoichiometry to 0.6 normal value	F_6
	Anode CO poisoning	H_2 supply subsystem	Feed hydrogen with 10 ppm CO	F_7
40-cell stack	Normal operating	Whole system	Nominal operation	<i>Normal</i>
	High current pulse	Electric circuit	Short circuit	F_3
	High temperature	Temperature subsystem	Stop cooling water	F_4
	High air stoichiometry	Air supply subsystem	Increase air stoichiometry to 2.2 normal value	F_5
	Low air stoichiometry	Air supply subsystem	Decrease air stoichiometry to 0.65 normal value	F_6

288 As the individual cell voltages were used as the variables for diagnosis,
289 the dimensional number of the original data was equal to the cell number in
290 the concerned stack. By using the FDA method, the features were extracted
291 from the original data. A part of extracted features are shown in Fig. 7(a),
292 Fig. 7(b) and Fig. 7(c). From these figures, it can be seen that the features in
293 normal state and different faulty states are generally separated in the lower
294 dimensional feature space. The characteristic lightens the computational
295 burden and improves the performance of the classification following feature
296 extraction step [37].

297 In a diagnosis cycle, classification is conducted in the feature space follow-
298 ing the feature extraction procedure. SSM-SVM, combined with the diagnos-
299 tic rule, is implemented in this phase. To construct the SSM-SVM classifier,
300 the radial basis function (RBF) was selected as the “kernel function”, and
301 parameters including the penalty factor and kernel parameter were optimized
302 based on the test database.

303 *6.1. Diagnosis accuracy*

304 We evaluated the online implementation results using two criteria: false
305 alarm rate (FAR) which is the rate of the samples in normal state wrongly
306 diagnosed into the faulty classes, and the diagnosis accuracy of each specific
307 fault type. According to the recorded diagnosed results, FAR reaches respec-
308 tively 2.82%, 0%, 2.09% for the three stacks, which exhibits a low level. The
309 diagnosis accuracies of the 7 fault types concerned are listed in Table 4. It
310 should be noted that the parameters are maintained at a high level ($> 95\%$)
311 for most fault types (F_1, F_2, F_4, F_5, F_7). The mis-classifications happened
312 mostly on the data in F_6 (low air stoichiometry fault) state, in which the cell

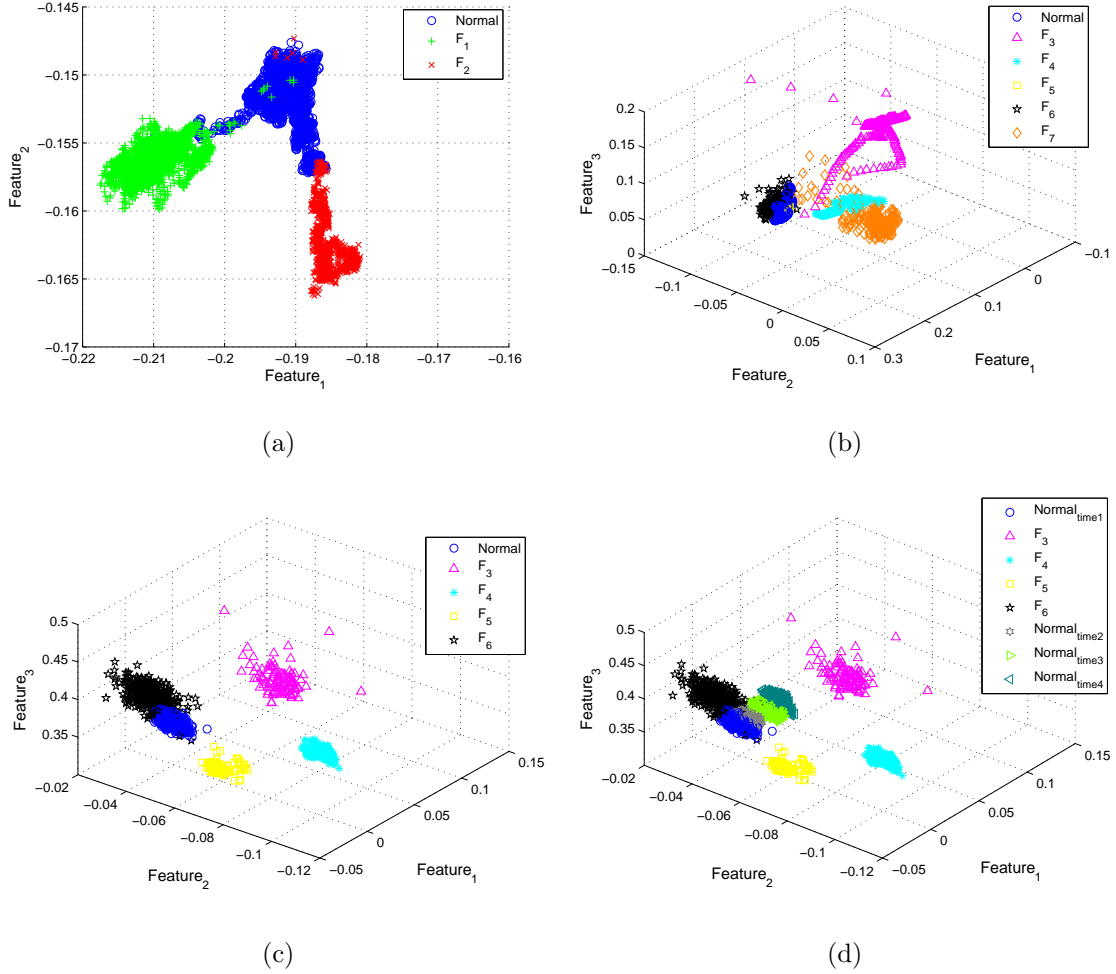


Figure 7. Features extracted from data of cell voltages. Normal, F_1 , F_2 , F_3 , F_4 , F_5 , F_6 and F_7 represent respectively the normal state, membrane drying fault, flooding fault, high current pulse fault, cooling water stopping fault, high air stoichiometry, low air stoichiometry, and anode CO poisoning. (a) 2-dimensional features extracted from the data in normal, F_1 and F_2 faulty states for a 20-cell stack. (b) 3-dimensional features extracted from normal and 5 various faulty states for a 8-cell stack. (c) 3-dimensional features extracted from normal and 4 various faulty states for a 40-cell stack. (d) 3-dimensional features extracted from normal state and 4 various faulty states for a 40-cell stack. The data in normal state (denoted as $Normal_{time1}$, $Normal_{time2}$, $Normal_{time3}$, $Normal_{time4}$) are sampled at different time points.

313 voltages show vary slightly compared with those in normal state. We also
 314 observe that the wrongly diagnosed data are mostly distributed in the initial
 315 stage of the fault where the data are located in the transition zone between
 316 clear normal state and faulty states.

Table 4. Diagnosis accuracy for different faults for different PEMFC stacks

Fault	F_1	F_2	F_3	F_4	F_5	F_6	F_7
Stack 1 (20-cell)	94.01%	99.21%	-	-	-	-	-
Stack 2 (8-cell)	-	-	91.63%	95.02%	100.00%	89.44%	99.08%
Stack 3 (40-cell)	-	-	93.55%	100.00%	99.56%	85.14%	-

F_1 : Membrane drying fault; F_2 : Flooding fault; F_3 : High current pulse fault; F_4 :
 Cooling water stopping fault; F_5 : High air stoichiometry; F_6 : Low air stoichiometry;
 F_7 : Anode CO poisoning.

317 6.2. Online computational complexity

318 Since the diagnosis approach is implemented using the ASIC whose com-
 319 puting capability and storage capacity are limited compared with a standard
 320 PC, the online computational complexity of the algorithm needs to be eval-
 321 uated. In our approach, the needed memories are respectively $O(ML)$ and
 322 $O(LS)$ for saving the trained feature extraction and classification models, in
 323 which S is the number of support vectors, while the online computing times
 324 are $O(ML)$ and $O(LS)$ for implementing the feature extraction and classifi-
 325 cation methods. From our test, the occupied memory is less than 200 kb for
 326 saving the parameters for diagnosis, while the online implementing time of a
 327 diagnosis cycle can be maintained at the level of 10 ms using the developed

328 ASIC. In our platforms, the sample time was set to 1 s, which means the
329 diagnosis cycle can be achieved by a large margin. To our knowledge, the
330 diagnosis cycle obtained in our test could satisfy the requirements for most
331 fuel cell systems.

332 *6.3. Novel fault mode recognition*

333 Conventional classification methods can only be used to recognize the
334 known faults which have been shown in the training database. When an
335 example from a new fault mode is treated, it will be diagnosed wrongly into
336 a known fault class or the normal one. We propose here the modified SVM
337 and diagnostic rule to overcome this shortcoming. To verify the proposal,
338 we assumed that a fault is unknown in the training process, and occurs in
339 the diagnosis stage. Taking the case of a 40-cell stack as example, when F_3 ,
340 F_4 , F_5 , F_6 were considered as the unseen fault, the probabilities that they
341 were successfully recognized as a novel fault mode are respectively 96.77%,
342 100.00%, 95.36%, 39.86% which are at a high level except the case of F_6 .
343 This results from the fact that the data in F_6 are too close to the normal
344 ones. They are mostly classified into the normal state class.

345 *6.4. Online adaptation*

346 In consideration of the ageing effects, the performance of the PEMFC
347 degrades with time. It results that the variables measured in the normal op-
348 erating state are non-stationary, i.e. the cell voltages decrease to some degree
349 after a period of time operation. Accordingly, the location of data in normal
350 state varies in the feature space (Fig. 7(d)). In this case, the initially trained
351 diagnosis approach may gradually lose its efficiency, i.e., the FAR increases.

352 To maintain the performance, we propose here an online adaptation method.
353 The online adaptation is realized via incremental learning of the SSM-SVM
354 classifier. We tested the diagnosis approach with and without online adapta-
355 tion during long-term operation. The 1st, 2nd, and 3rd tests were carried out
356 respectively at three different time points (the 20th day, 80th day, 170th day
357 counting from the beginning of the test). With the initially trained diagnosis
358 model (without online adaptation), the FARs obtained at the 1st, 2nd, and
359 3rd tests were respectively 35.5%, 100%, and 100%. This means that more
360 and more data in normal state were diagnosed as the faulty ones if we did not
361 modify the initially trained model. By contrast, with our proposed online
362 adaptation method, the FARs obtained at the 1st, 2nd, and 3rd tests were
363 respectively 0.25%, 0%, and 0%. The performance of the diagnosis approach
364 was therefore maintained.

365 *6.5. Discussion*

366 The data studied in this paper were acquired from the stacks operated in
367 nominal steady state. In some applications such as fuel cell vehicles, dynamic
368 operating conditions should be handled in diagnosis. In these cases, the
369 correlations of the samples could be considered. To achieve this, data series
370 instead of single data sample could be treated as the objects for classification
371 [39].

372 Data-driven diagnosis approach is focused on in this study to coordinate
373 with the cell voltage measurement. The proposed approach can be combined
374 with some model-based techniques to handle the system dynamics and to
375 improve the generalization capability. Hybrid diagnosis approach could be
376 one promising solution for fuel cell diagnosis [40].

377 The proposed data-driven approach is supposed to be applied jointly with
378 the developed ASIC. Although in the current commercial PEMFC systems, it
379 is not easy to measure individual cell voltages. We believe that the proposal
380 can be interesting for many fuel cell suppliers and can be a potential solution
381 in their future products.

382 **7. Conclusion**

383 In this study, we firstly propose the criteria for online fuel cell online di-
384 agnosis. To attain these criteria, we experimentally demonstrated an online
385 fault diagnosis strategy for PEMFC systems. With the specifically designed
386 ASIC, the proposed diagnosis approach was implemented online to diagnose
387 multiple faults with respect to several PEMFC stacks. We proposed here to
388 monitor the individual fuel cell voltages and employ them as the variables for
389 diagnosis. In contrast to most of the available approaches in which the fuel
390 cell voltages are assumed to be identical, the inhomogeneity among cells was
391 utilized and dedicated to fault diagnosis. From a fundamental point of view,
392 different faults can cause different thermal, fluidic, electrochemical spatial
393 distributions and these can be reflected by the amplitudes of individual cell
394 voltages. In this study, it was proved that the individual cell voltages pos-
395 sess the discriminative information of different health states. The importance
396 of monitoring every cell voltage, or several of them together, was therefore
397 stressed. From the diagnostic results of online validation, the diagnosis accu-
398 racy can be maintained at a high level with respect to different types of fault
399 and for different fuel cell stacks thanks to the utilization of FDA and SVM
400 methods. Besides, the capabilities of recognition an unseen faulty mode and

401 online adaptation, which the traditional diagnosis methods are not capable
402 of handling, were installed into our approach. The efficiency of the ASIC
403 that we designed here, which is dedicated to precisely measuring and online
404 implementing the diagnosis algorithm, was validated. The ASIC therefore
405 promises to be used as a routine component for monitoring fuel cell voltage
406 and implementing the diagnosis approach we proposed here.

407 Several directions can be interesting on fuel cell diagnosis. First, more
408 general system model should be built in consideration of different faulty
409 conditions. Second, more advanced data-based techniques can be applied to
410 improve the adaptability of the diagnosis methods. Third, the fault diagnosis
411 should be combined with control strategy to improve the fuel cells' reliability
412 finally.

413 **References**

- 414 [1] J. Wang, Barriers of scaling-up fuel cells: Cost, durabil-
415 ity and reliability, *Energy* 80 (2015) 509 – 521. doi:<http://dx.doi.org/10.1016/j.energy.2014.12.007>.
416 URL <http://www.sciencedirect.com/science/article/pii/S0360544214013644>
418
- 419 [2] L. Dubau, L. Castanheira, F. Maillard, M. Chatenet, O. Lottin,
420 G. Maranzana, J. Dillet, A. Lamibrac, J.-C. Perrin, E. Moukheiber,
421 et al., A review of PEM fuel cell durability: materials degradation, local
422 heterogeneities of aging and possible mitigation strategies, *Wiley Inter-*
423 *disciplinary Reviews: Energy and Environment* 3 (6) (2014) 540–560.
- 424 [3] R. Borup, J. Meyers, B. Pivovar, Y. S. Kim, R. Mukundan, N. Garland,
425 D. Myers, M. Wilson, F. Garzon, D. Wood, et al., Scientific aspects
426 of polymer electrolyte fuel cell durability and degradation, *Chemical*
427 *reviews* 107 (10) (2007) 3904–3951.
- 428 [4] Z. Zheng, R. Petrone, M. Péra, D. Hissel, M. Becherif, C. Pianese,
429 N. Yousfi Steiner, M. Sorrentino, A review on non-model based
430 diagnosis methodologies for PEM fuel cell stacks and systems, *Inter-*
431 *national Journal of Hydrogen Energy* 38 (21) (2013) 8914–8926.
432 doi:[10.1016/j.ijhydene.2013.04.007](http://dx.doi.org/10.1016/j.ijhydene.2013.04.007).
433 URL <http://linkinghub.elsevier.com/retrieve/pii/S0360319913008550>
434
- 435 [5] G. Tian, S. Wasterlain, I. Endichi, D. Candusso, F. Harel, X. Fra-

- 436 nois, M.-C. Péra, D. Hissel, J.-M. Kauffmann, Diagnosis meth-
437 ods dedicated to the localisation of failed cells within PEMFC
438 stacks, *Journal of Power Sources* 182 (2) (2008) 449 – 461.
439 doi:<http://dx.doi.org/10.1016/j.jpowsour.2007.12.038>.
440 URL [http://www.sciencedirect.com/science/article/pii/
441 S0378775307027061](http://www.sciencedirect.com/science/article/pii/S0378775307027061)
- 442 [6] R. Petrone, Z. Zheng, D. Hissel, M. Pra, C. Pianese, M. Sorrentino,
443 M. Becherif, N. Yousfi-Steiner, A review on model-based diagnosis
444 methodologies for PEMFCs, *International Journal of Hydrogen En-
445 ergy* 38 (17) (2013) 7077 – 7091. doi:[http://dx.doi.org/10.1016/j.
446 ijhydene.2013.03.106](http://dx.doi.org/10.1016/j.ijhydene.2013.03.106).
- 447 [7] S. X. Ding, *Model-based fault diagnosis techniques*, Vol. 2013, Springer,
448 2008.
- 449 [8] A. Hernandez, D. Hissel, R. Outbib, Modeling and Fault Diagnosis of
450 a Polymer Electrolyte Fuel Cell Using Electrical Equivalent Analysis,
451 *IEEE Transaction on Energy Conversion* 25 (1) (2010) 148–160. doi:
452 [10.1109/TEC.2009.2016121](http://dx.doi.org/10.1109/TEC.2009.2016121).
- 453 [9] S. de Lira, V. Puig, J. Quevedo, A. Husar, LPV observer de-
454 sign for PEM fuel cell system: Application to fault detec-
455 tion, *Journal of Power Sources* 196 (9) (2011) 4298 – 4305.
456 doi:<http://dx.doi.org/10.1016/j.jpowsour.2010.11.084>.
457 URL [http://www.sciencedirect.com/science/article/pii/
458 S0378775310020756](http://www.sciencedirect.com/science/article/pii/S0378775310020756)

- 459 [10] S. Laghrouche, J. Liu, F. Ahmed, M. Harmouche, M. Wack, Adaptive
460 second-order sliding mode observer-based fault reconstruction for pem
461 fuel cell air-feed system, *Control Systems Technology*, IEEE Transactions
462 on 23 (3) (2015) 1098–1109. doi:10.1109/TCST.2014.2361869.
- 463 [11] T. Escobet, D. Feroldi, S. de Lira, V. Puig, J. Quevedo, J. Ri-
464 era, M. Serra, Model-based fault diagnosis in PEM fuel cell
465 systems, *Journal of Power Sources* 192 (1) (2009) 216 – 223.
466 doi:http://dx.doi.org/10.1016/j.jpowsour.2008.12.014.
467 URL [http://www.sciencedirect.com/science/article/pii/
468 S0378775308023288](http://www.sciencedirect.com/science/article/pii/S0378775308023288)
- 469 [12] S. Yin, Data-driven design of fault diagnosis systems, Ph.D.
470 thesis, Universität Duisburg-Essen, Fakultät für Ingenieurwis-
471 senschaften» Ingenieurwissenschaften-Campus Duisburg» Abteilung
472 Elektrotechnik und Informationstechnik» Automatisierung und kom-
473 plexe Systeme (2012).
- 474 [13] D. Hissel, D. Candusso, F. Harel, Fuzzy-Clustering Durability Diagno-
475 sis of Polymer Electrolyte Fuel Cells Dedicated to Transportation Ap-
476 plications, *IEEE Transactions on Vehicular Technology* 56 (5) (2007)
477 2414–2420.
- 478 [14] Z. Li, R. Outbib, S. Giurgea, D. Hissel, Diagnosis for pemfc sys-
479 tems: A data-driven approach with the capabilities of online adaptation
480 and novel fault detection, *Industrial Electronics*, IEEE Transactions on
481 62 (8) (2015) 5164–5174. doi:10.1109/TIE.2015.2418324.

- 482 [15] D. Hissel, M. C. Péra, J. M. Kauffmann, Diagnosis of automotive fuel
483 cell power generators, *Journal of Power Sources* 128 (2) (2004) 239–246.
484 doi:<http://dx.doi.org/10.1016/j.jpowsour.2003.10.001>.
- 485 [16] N. Yousfi-Steiner, D. Hissel, P. Moçotéguy, D. Candusso, Diagnosis of
486 polymer electrolyte fuel cells failure modes (flooding & drying out)
487 by neural networks modeling, *International Journal of Hydrogen En-
488 ergy* 36 (4) (2011) 3067–3075. doi:<http://dx.doi.org/10.1016/j.ijhydene.2010.10.077>.
- 490 [17] Y. Vural, D. B. Ingham, M. Pourkashanian, Performance prediction
491 of a proton exchange membrane fuel cell using the ANFIS model,
492 *International Journal of Hydrogen Energy* 34 (22) (2009) 9181–9187.
493 doi:[10.1016/j.ijhydene.2009.08.096](http://dx.doi.org/10.1016/j.ijhydene.2009.08.096).
- 494 [18] J. Hua, J. Li, M. Ouyang, L. Lu, L. Xu, Proton exchange membrane
495 fuel cell system diagnosis based on the multivariate statistical method,
496 *International Journal of Hydrogen Energy* (2011) 1–10doi:[10.1016/j.ijhydene.2011.05.075](http://dx.doi.org/10.1016/j.ijhydene.2011.05.075).
497 URL <http://dx.doi.org/10.1016/j.ijhydene.2011.05.075>
- 499 [19] Z. Zheng, M.-C. Péra, D. Hissel, M. Becherif, K.-S. Ag-
500 bli, Y. Li, A double-fuzzy diagnostic methodology dedicated
501 to online fault diagnosis of proton exchange membrane fuel
502 cell stacks, *Journal of Power Sources* 271 (2014) 570 – 581.
503 doi:<http://dx.doi.org/10.1016/j.jpowsour.2014.07.157>.
504 URL [http://www.sciencedirect.com/science/article/pii/
505 S0378775314012117](http://www.sciencedirect.com/science/article/pii/S0378775314012117)

- 506 [20] L. Alberto, M. Riascos, M. G. Simoes, P. E. Miyagi, On-line fault diag-
507 nostic system for proton exchange membrane fuel cells, *Journal of Power*
508 *Sources* 175 (2008) 419–429.
- 509 [21] S. Wasterlain, D. Candusso, F. Harel, X. François, D. Hissel, Diagno-
510 sis of a fuel cell stack using electrochemical impedance spectroscopy
511 and bayesian networks, in: *Vehicle Power and Propulsion Conference*
512 *(VPPC)*, 2010 IEEE, 2010, pp. 1–6. doi:10.1109/VPPC.2010.5729184.
- 513 [22] J. Chen, B. Zhou, Diagnosis of PEM fuel cell stack dynamic behaviors,
514 *Journal of Power Sources* 177 (1) (2008) 83 – 95. doi:http://dx.doi.
515 org/10.1016/j.jpowsour.2007.11.038.
- 516 [23] N. Y. Steiner, D. Hissel, P. Moçotéguy, D. Candusso, Non intrusive
517 diagnosis of polymer electrolyte fuel cells by wavelet packet transform,
518 *International Journal of Hydrogen Energy* 36 (1) (2011) 740 – 746.
519 doi:http://dx.doi.org/10.1016/j.ijhydene.2010.10.033.
520 URL [http://www.sciencedirect.com/science/article/pii/
521 S0360319910021129](http://www.sciencedirect.com/science/article/pii/S0360319910021129)
- 522 [24] D. Benouioua, D. Candusso, F. Harel, L. Oukhellou, Fuel cell diag-
523 nosis method based on multifractal analysis of stack voltage signal,
524 *International Journal of Hydrogen Energy* 39 (5) (2014) 2236 – 2245.
525 doi:http://dx.doi.org/10.1016/j.ijhydene.2013.11.066.
526 URL [http://www.sciencedirect.com/science/article/pii/
527 S0360319913027912](http://www.sciencedirect.com/science/article/pii/S0360319913027912)
- 528 [25] E. Monmasson, M. Cirstea, *FPGA Design Methodology for Industrial*

- 529 Control Systems—A Review, *Industrial Electronics*, *IEEE Transactions*
530 on 54 (4) (2007) 1824–1842. doi:10.1109/TIE.2007.898281.
- 531 [26] C. Steiger, H. Walder, M. Platzner, Operating systems for reconfigurable
532 embedded platforms: online scheduling of real-time tasks, *Computers*,
533 *IEEE Transactions on* 53 (11) (2004) 1393–1407. doi:10.1109/TC.
534 2004.99.
- 535 [27] P. Rodatz, F. Bchi, C. Onder, L. Guzzella, Operational as-
536 pects of a large PEFC stack under practical conditions, *Journal of Power Sources* 128 (2) (2004) 208 – 217. doi:http:
537 //dx.doi.org/10.1016/j.jpowsour.2003.09.060.
538 URL [http://www.sciencedirect.com/science/article/pii/
539 S0378775303010085](http://www.sciencedirect.com/science/article/pii/S0378775303010085)
540
- 541 [28] Z. Li, R. Outbib, S. Giurgea, D. Hissel, Y. Li, Fault detection and iso-
542 lation for polymer electrolyte membrane fuel cell systems by analyzing
543 cell voltage generated space, *Applied Energy* 148 (2015) 260 – 272.
544 doi:http://dx.doi.org/10.1016/j.apenergy.2015.03.076.
545 URL [http://www.sciencedirect.com/science/article/pii/
546 S0306261915003682](http://www.sciencedirect.com/science/article/pii/S0306261915003682)
- 547 [29] E. Gerstner, Nobel prize 2007: Fert and grünberg, *Nature Physics* 3 (11)
548 (2007) 754–754.
- 549 [30] Y. S. Chai, S. Kwon, S. H. Chun, I. Kim, B.-G. Jeon, K. H. Kim, S. Lee,
550 Electrical control of large magnetization reversal in a helimagnet, *Nature*
551 *communications* 5.

- 552 [31] Z. Li, R. Outbib, D. Hissel, S. Giurgea, Data-driven diagnosis of PEM
553 fuel cell: A comparative study, *Control Engineering Practice* 28 (2014)
554 1–12. doi:10.1016/j.conengprac.2014.02.019.
555 URL [http://linkinghub.elsevier.com/retrieve/pii/
556 S0967066114001002](http://linkinghub.elsevier.com/retrieve/pii/S0967066114001002)
- 557 [32] G. McLachlan, *Discriminant analysis and statistical pattern recognition*,
558 Vol. 544, John Wiley & Sons, 2004.
- 559 [33] J. C. Platt, *Sequential Minimal Optimization : A Fast Algorithm for*
560 *Training Support Vector Machines*, Technical Report MSR-TR-98-14,
561 Microsoft Research (1998) 1–21.
- 562 [34] P. Y. Hao, Y. H. Lin, A new multi-class support vector machine with
563 multi-sphere in the feature space, in: *Proceedings of the 20th interna-*
564 *tional conference on Industrial, engineering, and other applications of*
565 *applied intelligent systems, IEA/AIE'07*, Springer-Verlag, Berlin, Hei-
566 delberg, 2007, pp. 756–765.
- 567 [35] P. Freitas, R. Ferreira, S. Cardoso, F. Cardoso, Magneto-resistive sensors,
568 *Journal of Physics: Condensed Matter* 19 (16) (2007) 165221.
- 569 [36] M. Pannetier-Lecoecur, C. Fermon, A. Giraud, GMR based integrated
570 non-contact voltage sensor for fuel cells monitoring, in: *Sensing Technol-*
571 *ogy (ICST), 2011 Fifth International Conference on*, 2011, pp. 101–105.
572 doi:10.1109/ICSensT.2011.6136941.
- 573 [37] Z. Li, S. Giurgea, R. Outbib, D. Hissel, Online Diagnosis of PEMFC
574 by Combining Support Vector Machine and Fluidic Model, *Fuel Cells*

- 575 14 (3) (2014) 448–456. doi:10.1002/fuce.201300197.
576 URL <http://doi.wiley.com/10.1002/fuce.201300197>
- 577 [38] C. de Beer, P. S. Barendse, P. Pillay, Fuel Cell Condition Monitoring
578 Using Optimized Broadband Impedance Spectroscopy, *IEEE Transac-*
579 *tions on Industrial Electronics* 62 (8) (2015) 5306–5316. doi:10.1109/
580 TIE.2015.2418313.
- 581 [39] Z. Li, R. Outbib, S. Giurgea, D. Hissel, Fault diagnosis for pemfc systems
582 in consideration of dynamic behaviors and spatial inhomogeneity, *IEEE*
583 *Transactions on Energy Conversion* (2018) 1–1doi:10.1109/TEC.2018.
584 2824902.
- 585 [40] Z. Li, R. Outbib, D. Hissel, S. Giurgea, Diagnosis of pemfc by using
586 data-driven parity space strategy, in: *2014 European Control Conference*
587 *(ECC)*, 2014, pp. 1268–1273. doi:10.1109/ECC.2014.6862527.